Bubbles in the Hele-Shaw cell: Pattern selection and tip perturbations

Daniel C. Hong* and Fereydoon Family
Department of Physics, Emory University, Atlanta, Georgia 30322
(Received 18 March 1988)

We consider the motion of a symmetric finite bubble in a two-dimensional Hele-Shaw cell. In the absence of surface tension, the Saffman-Taylor solution contains two free parameters, U and λ, for a given bubble area J, where U is the dimensionless speed and λ is the dimensionless width of the bubble. It is shown that, in the presence of surface tension, a solution does not exist for $U>2$ for any bubble area. We also derive the following scaling relations: (a) $2-U\approx\epsilon^{2/3}$ for large J; and (b) $2-U\approx\epsilon^{2}$ for small J, where ϵ is a small parameter which is proportional to the surface tension. We show that by creating a cusp at the tip of the bubble, one can increase the speed of the bubble $U>2$. We present predictions for the shape and speed of the symmetric bubble as a function of the external parameters in the presence of a cusp at the tip. This picture may explain the recent experimental results of Maxworthy, where substantially enhanced velocities were measured for the anomalous bubbles with a tiny bubble at the tip.

I. INTRODUCTION

Fluid motion in a two-dimensional Hele-Shaw cell has received renewed interest in recent years.[1] Attention has focused on the selection mechanism of a finger width that forms in the Hele-Shaw cell.[2] The problem of predicting the width of a steady-state finger turns out to be mathematically similar to the selection mechanism of the dendrite growing in the undercooled melt; in the absence of surface tension, both problems possess a continuous family of solutions. Surface tension breaks this continuous family into a discrete set among which only one state is dynamically stable and thus selected.[2-6]

A less studied but closely related problem is the motion of a finite bubble in a Hele-Shaw cell.[7-11] Consider a finite bubble in a Hele-Shaw cell which is initially filled with fluid of higher viscosity. The question is: What will be the shape and the speed of the bubble if we push the fluid from far left with the rate VW per second, where V is the velocity and W is the size of the wall? Taylor and Saffman[7] worked out this problem in the absence of surface tension and discovered that for a given bubble area, the speed of the bubble is undetermined; its speed can vary from V to infinity. Experimentally, however, unique velocity is selected.[11] This problem is similar in spirit to the Saffman-Taylor problem, where the width of the finger is undetermined. We thus expect that a similar mechanism discovered in the Saffman-Taylor problem should work; surface tension breaks the continuous family into a discrete set. Recently Tanveer[10] studied this problem with a finite surface tension and indeed found that the continuous family breaks into a discrete set. Moreover, he numerically found that, regardless of the bubble size, the speed of the bubble never exceeds twice that of the pushing fluid. This is quite similar to what happens in the Saffman-Taylor problem where solutions with the dimensionless width $\lambda<\frac{1}{2}$ are not allowed because they create an unphysical cusp at the tip. The first purpose of this paper is to show how the limit $2V$ arises naturally if we impose a smooth boundary condition everywhere on the finite surface. We also predict scaling relations between U and V as a function of the external parameters.

The second question to be addressed in this paper is motivated by the recent experiment performed by Maxworthy.[11] He studied the motion of a rising bubble to the tip of which a tiny bubble was attached in a two-dimensional Hele-Shaw cell in the presence of the gravitational field. He found that the rising velocity of these bubbles is five to ten times that of ordinary bubbles, which is significantly larger than the limit $2V$ found by Tanveer.[10] The size of the tiny bubble is insignificant in comparison with that of the rising bubble, yet the effect on the shape as well as to the rising velocity is dramatic. This discovery is the same as what was observed by Couder, Gerard, and Rabaud[12] who injected a tiny bubble at the tip of the growing finger in the Hele-Shaw and found narrow fingers with $\lambda<\frac{1}{2}$. Recently a model was presented to understand Couder's experiment from the view point of the solvability theory[3] based on the idea that the bubble creates a cusp at the tip and maintains it by sitting there.

In this paper we extend the solvability theory developed for Couder's finger to Maxworthy's anomalous bubble. Our goal is to develop an understanding of the anomalous velocity enhancement caused by a tip perturbation within the framework of the solvability theory. We also present some theoretical predictions which can be tested experimentally. This paper is organized as follows. In Sec. II we first write down the solvability conditions for the finite bubble in the presence of surface tension and then derive scaling relations between the speed of the bubble and external parameters which includes surface tension. We will show that solutions cannot exist for $U>2V$, where U is the speed of the bubble. We then show in Sec. III how the anomolous velocity enhancement due to the tiny bubble can be understood within the framework of solvability theory.

II. SOLVABILITY CONDITIONS FOR A FINITE BUBBLE

This section is primarily concerned with the derivation of the solvability conditions for a symmetric finite bubble moving in a two-dimensional Hele-Shaw cell. We start our analysis by first defining the geometry of the cell and the governing equations of motion. The cell is made of two infinitely long glass plates with width $2W$, which is vertically a distance $b \ll W$ apart and thus is an effectively two-dimensional cell. The side walls of the cell is blocked and the motion of the fluid is confined along the x direction. The cell is filled with fluid of finite viscosity μ and a bubble with finite area is injected along the center of the cell. We then push the fluid from left and extract it from right with the rate $2VW$ per second. In what follows we set $V=1$. The bubble moves with speed U which is in general greater than 1. Also the bubble adjusts its shape and has a unique width λ as shown in Fig. 1. Parameters U and λ are experimentally measurable quantities and thus one should be able to predict their behavior as a function of the external parameters. To this end we first write down the equations of motion for the bubble. The velocity v satisfies Darcy's law everywhere inside the cell,

$$v=\frac{b^2}{12\mu}\nabla p=\nabla\phi \ , \tag{2.1}$$

where p is the pressure and ϕ is the velocity potential. The fluid is incompressible and the velocity potential ϕ will satisfy the Laplace equation

$$\nabla^2\phi=0 \ . \tag{2.2}$$

Two boundary conditions must be satisfied at the surface of the finger surface,

$$v_n=\frac{\partial\phi}{\partial n} \ , \tag{2.3}$$

where v_n is the normal velocity of the finger surface and the derivative is taken along the normal direction, and

$$\phi_s=\frac{b^2\gamma\kappa}{12\mu} \ , \tag{2.4}$$

where ϕ_s is the value of ϕ at the surface and κ is the curvature. There is one more boundary condition to be satisfied at the side walls. Since the walls are blocked, fluid cannot flow out and thus the normal velocity must vanish at the side walls. This implies that if the bubble is finite then the velocity field at infinity should not be affected and

$$v=V \text{ at } x=\pm\infty \ . \tag{2.5}$$

In the absence of surface tension γ, the above equations can be solved exactly as was done by Taylor and Saffman 30 years ago.[7] Their solutions contain two parameters λ and U and there is no way to select these two parameters uniquely without surface tension. In the presence of surface tension, the solutions to Eqs. (2.3)–(2.5) cannot be obtained in a closed form since this involves solving a highly nonlinear and nonlocal integrodifferential equation. Therefore the natural way of solving the above equations is to introduce the surface tension perturbatively. This can be justified as long as the capillary length induced by the surface tension is small. Capillary length d_0 is defined as a length scale at which the perturbation on the finger surface is marginally stable. Simple linear stability analysis[7] in the presence of surface tension gives the capillary length in terms of the external parameters

$$d_0=(b^2\gamma/12W^2\mu v)^{1/2} \tag{2.6}$$

which is of the order of 10^{-4} and is small enough that a perturbation approach is justified. There is, however, a subtlety in doing this because surface tension acts as a singular perturbation. The effect of surface tension on the finger surface is exponentially small and can be safely ignored. However, this tiny term is responsible for the selection mechanism.[2–6] The predictions of this scenario have been tested in both numerical experiments[13] and real experiment[3,12,14] for a variety of patterns. One expects that the same approach can be applied to this problem as well. Tanveer[9,10] recently included surface tension in his analysis and indeed found that unique velocity and shape are selected in the presence of surface tension. In this paper we recast his equation of motion into a linear second-order integrodifferential equation and explicitly write down the solvability conditions. After a little bit of tedious, but straightforward algebra, one obtains the following linear integrodifferential equation for the first-order shape correction $\zeta_1=\zeta-\zeta_0$, where ζ is the true shape, and ζ_0 the Saffman-Taylor zero surface-tension solution:

$$\epsilon\frac{d^2\zeta_1}{d\eta^2}+\epsilon P_0(\eta)\frac{d^2\zeta_2}{d\eta^2}+\epsilon P_1(\eta)\frac{d\zeta_1}{d\eta}+\epsilon P_2(\eta)\frac{d\zeta_2}{d\eta}+Q(\eta)\zeta_1=R(\eta) \ , \tag{2.7}$$

where ζ_2 is the Hilbert transform of ζ_1 and

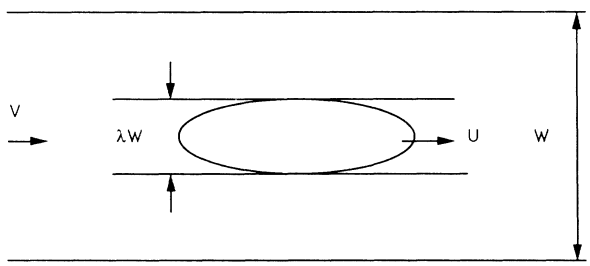

FIG. 1. Top view of the two-dimensional Hele-Shaw cell. The cell is filled with fluid of viscosity μ and a bubble is injected along the center. The fluid is pushed from the left with a rate WV per second. V is set to 1. The bubble is moving with a relative velocity $U>1$ and the dimensionless width of the bubble is denoted as λ. For a given bubble area, U and λ are not uniquely determined in the absence of surface tension.

$$P_0(\eta)=-\eta\ , \tag{2.8a}$$

$$P_1(\eta)=\frac{2\eta}{\delta^2+\eta^2}+\frac{S_1(\eta)(1+\eta^2/\delta^2)}{\delta(1+\delta^2)^2}\ , \tag{2.8b}$$

$$P_2(\eta)=\frac{2\eta}{\delta^2+\eta^2}+\frac{S_2(\eta)(1+\eta^2/\delta^2)}{\delta(1+\eta^2)^2}\ , \tag{2.8c}$$

$$S_1(\eta)=-\frac{\eta}{8}+\frac{8\alpha^2\eta}{\delta[(1+\alpha^2)^2(1+\eta^2/\delta^2)-4\alpha^2]}+\frac{2\delta[(1-\alpha^2)^2-(1+\alpha^2)(U-1)^2]\eta}{(1+\alpha^2)^2(U-1)^2(1+\eta^2)}\ , \tag{2.8d}$$

$$S_2(\eta)=-\eta S_1(\eta)-\delta(1+\eta^2/\delta^2)\ , \tag{2.8e}$$

$$Q(\eta)=\frac{4(1+\eta^2)^{3/2}}{(1-\alpha^2)^2(U-1)^2[1+\eta^2/(U-1)^2](1+\eta^2/\delta^2)^2}\ , \tag{2.8f}$$

$$R(\eta)=-\frac{\epsilon}{(1+\eta^2/\delta^2)^2}[G_1(\eta)+G_2(\eta)]\ , \tag{2.8g}$$

$$G_1(\eta)=\frac{1}{(1+\alpha^2)(U-1)^2}\frac{2(1-\eta^2/\delta^2)(1+\eta^2/\delta)[U(1+\alpha^2)-2\alpha^2]}{\eta(1+\eta^2/\delta^2)^{3/2}}\ , \tag{2.8h}$$

$$G_2(\eta)=\frac{4(1-\alpha^2)[U(1+\alpha^2)-2\alpha^2]\eta^2(1+\eta^2/\delta^2)[U(1+\alpha^2)-2\alpha^2]}{(1+\alpha^2)^4(U-1)^4\{1-(1-\alpha^2\eta^2)/[1+\alpha^2(U-1)^2]\}(1+\eta^2/\delta^2)^{3/2}}\ , \tag{2.8i}$$

and the small parameters ϵ and δ are defined as

$$\epsilon=\frac{b^2\gamma\pi^2U}{48\mu W^2\alpha^2}\ \text{and}\ \delta=\frac{1+\alpha^2}{1-\alpha^2}(U-1)\ . \tag{2.9}$$

For zero surface tension, Saffman-Taylor found a continuous family of solutions for a given bubble area, where the speed U, the dimensionless width λ, and the area of the bubble are related to α as

$$\alpha=\tan\left[\frac{\pi U\lambda}{4}\right]\ \text{and}\ J=\frac{8(U-1)}{\pi^2U}\ln\left[\frac{1+\alpha^2}{1-\alpha^2}\right]\ . \tag{2.10}$$

For a given bubble area J, (2.10) provides a relation between U and λ but no selection is made. As will be seen, surface tension breaks the continuous family of solutions into a discrete set and one of them is selected. Once the speed of the bubble is selected, the width λ is automatically selected by (2.10) for a given bubble area.

The variable η in (2.7) is the tangential slope of the zero surface-tension solution which varies from $-\infty$ to $+\infty$ as we move from the center of the lower boundary to that of the upper boundary crossing the tip at the right. In the presence of an inhomogeneous term, (2.7) still resists in yielding closed form solutions. We now follow the standard procedure of selecting solutions out of continuous family of solutions: We first construct an adjoint operator to the homogeneous part of (2.7) and then employ the Wentzel-Kramers-Brillouin (WKB) technique to find solutions to this adjoint equation (these two solutions will be called null eigenvectors). Then the necessary conditions for the existence of solutions will be to state that these two null eigenvectors should be orthogonal to the inhomogeneous term. The essential physics via solvability condition will crucially depend on functions $P_0(\eta)$ and $Q(\eta)$. The other functions only make the algebra complicated without changing the essential physics.[2–6] Therefore in this work we will neglect the first-order terms in (2.7) and consider the following simplified equation of motion:

$$\epsilon\frac{d^2Z}{d\eta^2}+\epsilon P_0(\eta)\frac{d^2Z}{d\eta^2}+Q(\eta)Z=R(\eta)\ , \tag{2.11}$$

where again Z is the Hilbert transform of Z and $R(\eta)$ is a smooth even function whose detailed form is not important. When (2.11) is solvable, then (2.7) is solvable, too. We now construct WKB solutions to the above equation.[3,4] We assume that solutions are of the form

$$Z=\exp[S_0(\eta)/\sqrt{\epsilon}]\ . \tag{2.12}$$

In the limit of small ϵ, we deform the contour of integration in Eq. (2.11) into the complex plane. The magnitude of real part of S_0 must decrease in the direction of deforming the contour in order to ensure that the integral exists. Then the main contribution to the integral will come from the pole in the real axis and can be evaluated simply using residue theorem.[4] We then end up with the following equation for the two null eigenvectors, $Z_\pm$:

$$\epsilon\frac{d^2Z_\pm}{d\eta^2}+Q(\eta)Z_\pm=0\ , \tag{2.13}$$

where

$$Q(\eta)=\frac{4(1+\alpha^2)^2(U-1)^2(1\pm i\eta)^{3/4}(1\mp i\eta)^{1/4}}{(1+\Gamma_1\eta^2)(1+\Gamma_2\eta^2)^2} \tag{2.14a}$$

with

$$\Gamma_1=\frac{1-\alpha^2}{1+\alpha^2}\frac{1}{(U-1)^2}\ \text{and}\ \Gamma_2=\frac{1}{(U-1)^2}\ . \tag{2.14b}$$

Equation (2.13) is now an ordinary second-order differential equation and its WKB solutions can be easily constructed and have the form

$$Z_\pm=\exp\left[i\frac{1}{\sqrt{\epsilon}}\int_0^\eta d\eta'\Psi(\eta')\right] \tag{2.15}$$

with

$$\Psi(\eta)=\frac{2}{(U-1)(1+\alpha^2)}\int_0^{\eta}d\eta\frac{(1\pm i\eta)^{4/3}(1\mp i\eta)^{1/4}}{(1+\Gamma_1\eta^2)^{1/2}(1+\Gamma_2\eta^2)}\ . \tag{2.16}$$

Note that $Z_+(\eta)=Z_-(\eta)^*$ and that the real and imaginary parts of $Z_+(\eta)$ are even and odd, respectively. We now write down the solvability condition,

$$\begin{aligned}\Pi&=\langle R(\eta)Z_+(\eta)\rangle\\&=\langle R(\eta)Z_-(\eta)\rangle^*\\&=\int_{-\infty}^{+\infty}d\eta\,R(\eta)\exp\left[i\frac{\Psi(\eta)}{\sqrt{\epsilon}}\right]\ .\end{aligned} \tag{2.17}$$

By symmetry, the imaginary part of Π will automatically vanish and thus we have only one solvability condition. The solvability condition is to state that Π should vanish. We now consider three distinct regimes: (a) the Saffman-Taylor finger limit, (b) the large limit, and (c) the small bubble limit.

A. Saffman-Taylor finger limit

The Saffman-Taylor finger limit corresponds to the limit $\alpha\to 1$ and, simultaneously, $U\lambda\to 1$. In this limit the solvability condition, (2.17) reduces to what was obtained previously.[3] The main prediction of Ref. 3 will be recovered: solutions do not exist for fingers of $\lambda<\frac{1}{2}$. For a finger with $\lambda>\frac{1}{2}$, λ satisfies the scaling relation $\lambda-\frac{1}{2}\approx\epsilon^{2/3}$.

B. Large bubble limit

Large bubbles correspond to the limit $\alpha\to 1$ and U finite. The dominant contribution to the integral of (2.17) will come from the neighborhood of the stationary phase of $\Psi(\eta)$ which has two stationary phases $\eta=\pm i$ with branch cuts. The branch points now depend on Γ_1 and Γ_2. Note that $0\le\alpha\le 1$ and thus $1/\Gamma_2\le 1/\Gamma_1$. If $U>2$, then the absolute value of $1/\Gamma_1$ is greater than 1. In this case the branch cuts run from $\eta=\pm i$ to $\pm i\infty$. The steepest descent path for Π will run from $-\infty$ to the stationary phase $\eta=i$ and then run away to $+\infty$. The solvability function Π will have the form

$$\Pi\approx N(\alpha,U,\epsilon)\exp\left[-\frac{1}{(U-1)(1+\alpha^2)}\frac{I_0(\alpha,U)}{\sqrt{\epsilon}}\right]\ , \tag{2.18}$$

where

$$I_0(\alpha,U)=2\int_0^1 dx\frac{(1-x)^{3/4}(1+x)^{1/4}}{(1-\Gamma_1x^2)^{1/2}(1-\Gamma_2x^2)} \tag{2.19}$$

and $N(\alpha,U,\epsilon)$ is a multiplicative constant which is given by

$$N(\alpha,U,\epsilon)\approx -N_0\epsilon^{9/7}\frac{U^{6/7}}{(U-2)^{43/14}(U-1)^{8/7}}\ \text{as}\ \alpha\to 1\ , \tag{2.19'}$$

$$N(\alpha,U,\epsilon)\approx -N_0'\epsilon^{9/7}\frac{(U-1)^{6/7}}{U^{1/7}(U-2)^{15/14}}\ \text{as}\ \alpha\to 0\ , \tag{2.19''}$$

with

$$N_0=\frac{\pi 2^{5/7}}{7^{3/4}\Gamma(\frac{3}{4})}\ \text{and}\ N_0'=\frac{2^{15/7}\pi}{7^{3/4}\Gamma(\frac{3}{4})}\ .$$

The solvability function Π will be always less than zero and thus no solution exists. This is the analytical explanation for the absence of the bubble solutions for $U>2$. Now for $U<2$, the stationary phase $\eta=i$ should be considered as a complex conjugate pair because of the logarithmic branch point at $\eta=i(U-1)$ produced by a term in the denominator. The function $\Psi(i)$ gains an imaginary term due to this extra branch cut. The δ steepest descent path now runs from $-\infty$ to $i-\delta$, with $\delta\ll 1$ running along the imaginary axis to $\eta=i(U-1)$ and coming back to $i+\delta$ and running away to $+\infty$. The contribution along the extra branch cut will now produce an extra term in the solvability function Π which is proportional to the cosine function. The argument of this cosine function will be just the discontinuity in $\Psi(i)$ across the cut. Simple residue theorem around this singular point produces an imaginary part in $\Psi(i)$,

$$[\Psi(i+\delta)-\Psi(i-\delta)]=\frac{\pi i}{[2(1+\alpha^2)]^{1/2}}\frac{(2-U)^{3/4}U^{1/4}}{\alpha}\quad\text{as}\ \delta\to 0\ . \tag{2.20}$$

The crossover from oscillating to nonoscillating state occurs when $\Psi(\eta)/\sqrt{\epsilon}$ changes by an amount of order unity as η moves from one side of the cut to the other at $\eta=i$. Thus by (2.20) we find

$$(2-U)\approx\epsilon^{2/3}\ . \tag{2.21}$$

C. Small bubble limit

Small bubbles correspond to the limit $\alpha\to 0$. Setting $\alpha=0$ in (2.16), we find

$$\frac{\Psi(\eta)}{\sqrt{\epsilon}}\approx\frac{2}{(U-1)}\frac{1}{\sqrt{\epsilon}}\int_0^{\eta}d\eta\frac{(1+i\eta)^{3/4}(1-i\eta)^{1/4}}{[1+\eta^2/(U-1)^2)]^{3/2}}\ . \tag{2.22}$$

In this limit again, no solution will exist for $U>2$ by the same reasoning applied to the large bubble limit. For $U<2$, the branch cut now extends from $\pm i$ to $\eta=\pm i(U-1)$ and the steepest descent path must include this section. If this section is long enough, then the solvability function Π will again oscillate and produce many zeros. In order to be more specific, we expand $\Psi(\eta)$ around the stationary phase $\eta=i$ for $|\omega|\ll 2-U\ll 1$,

$$\frac{\Psi(\eta)}{\sqrt{\epsilon}}-\frac{\Psi(i)}{\sqrt{\epsilon}}\approx -i\frac{2\sqrt{2}(U-1)^2}{7\sqrt{\epsilon}}\frac{\omega^{7/4}}{[U(2-U)]^{3/2}}\ . \tag{2.23}$$

The crossover from oscillating to nonoscillating occurs when the right-hand side of (2.23) becomes of the order of one at the branch point $\omega_b=2-U$; thus we obtain

$$(2-U)\approx\epsilon^2\ . \tag{2.24}$$

Predictions (2.21) and (2.24) are new and, in principle,

can be directly tested in the laboratory. There are some difficulties, however, as in the Saffman-Taylor experiment. The theory presented above is strictly two dimensional but in the real experiment one cannot ignore three-dimensional effects which will produce slight deviations from the theoretical predictions. For example, one will definitely observe a bubble with the speed $U>2$, which is forbidden in a strictly two-dimensional theory. In order to incorporate this three-dimensional effect, one should use different boundary conditions and this will not be addressed in this paper. For aspect ratio $b/w \ll 1$, the two-dimensional theory, however, will satisfactorily explain the experimental results. In the absence of experimental result, this remains to be seen.

III. TIP PERTURBATIONS

In this section we present an explanation for the experimental results of Maxworthy.[1] Maxworthy recently performed a series of experiments on rising bubbles in an effectively two-dimensional Hele-Shaw cell in the presence of a gravitational field. The gravitational field was introduced by tilting the cell. The effect of the gravitational field, however, can be eliminated by shifting the velocity field and the net effect is the same as pushing the background water with the modified speed which depends on the tilting angle, viscosity, and the gravitational field.[9] Therefore his experimental results appear to be relevant in checking our theoretical predictions of Sec. II. Unfortunately, however, his experimental results seem to indicate that two-dimensional formulation with Saffman-Taylor boundary conditions only hold in the limit of vanishing gravitational field. In this paper we do not want to investigate why this is so. Rather we are interested in his discovery of anomalous bubbles which rise with substantially enhanced velocities in comparison with ordinary bubbles.

Now let us examine Maxworthy's anomolous bubbles. Maxworthy provided a picture of his anomolous bubble in his paper which we have reproduced in Fig. 2. The bubble at the tip (hereafter at the tip is omitted) modifies the flow field around the tip and we do not have precise knowledge of this modified flow field. When we look at Maxworthy's photograph of the bubble, the tip is slightly pushed backward. If we ignore this tiny bubble and join both sides of the bubble boundary, we will find a cusp right at the tip. This cusp is responsible for the behavior of the anomolous bubbles. As was shown in Sec. II, the speed of the bubble without any external perturbation must be less than 2. For $U>2$, we have shown that the bubble must allow a cusp at the tip. Therefore the proposal in this paper is to assume that the effect of the bubble is to create a cusp at the tip and maintain it by staying there. When the rising velocity is large, the bubble trapped at the tip oscillates and produces an array of beautiful side branches. This paper is entirely focused on the steady-state pattern of anomolous bubbles, leaving dynamics for future study.

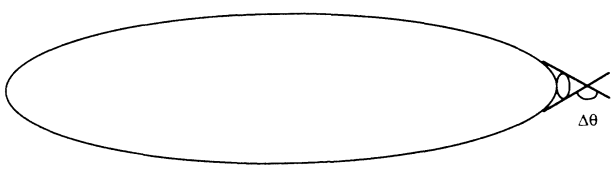

FIG. 2. Schematic picture of the bubble with a tiny bubble attached at the tip.

The starting point of our analysis is the previous observation that the tiny bubble at the tip creates a cusp. The strength of the cusp, called a mismatch angle $\Delta\theta$, is measured by the discontinuity in the tangential slope as usual. We rewrite (2.11) as follows:[3]

$$\epsilon\frac{d^2Z}{d\eta^2}+\epsilon P_0(\eta)\frac{d^2Z}{d\eta^2}+Q(\eta)Z(\eta) = R(\eta)+\epsilon f(\alpha,U)\Delta\theta(0)\delta(\eta)\ , \quad (3.1)$$

where

$$f(\alpha,U)=\left[\frac{dy}{d\eta}\right]_{y=0}=\frac{4\alpha}{(1+\alpha^2)(U-1)\pi U}\ . \quad (3.1')$$

In obtaining (3.1'), we have used the relations

$$y=(2/\pi U)\tan^{-1}[2\alpha\sin\theta/(1-\alpha^2)]$$

and $\eta=\delta\tan\theta$. Here again we omit the first-order terms in (2.7). Note that the additional term in the right hand side represents an amount of mismatch at the tip. This can be easily seen by integrating both sides twice across the tip. We now ask the solvability conditions for (2.25). Regarding the right-hand side of (3.1) as an inhomogeneous term, the null eigenvectors remain unchanged. Thus the solvability condition for Π defined in (2.17) is not zero but finite. After a little algebra, we obtain the relation between the mismatch angle $\Delta\theta$ and the solvability function Π. We find

$$\Delta\theta(0)\approx -N(\alpha,U,\epsilon)f(\alpha,U)\exp[-I_0(\alpha,U)/\sqrt{\epsilon}]\ , \quad (3.2)$$

where $N(\alpha,U,\epsilon)$ were defined in Eqs. (2.9') and (2.19'') for different α, and $f(\alpha,U)$ was defined in Eq. (3.1'). Since we omitted the first-order term in obtaining (3.2), $\Delta\theta(0)$ is not precise. This multiplicative factor, however, is not important as long as it is not zero. As we will see in what follows, what is important is an exponential factor in Eq. (3.2) which contains most of the information. The physical meaning of Eq. (3.2) becomes clear when we display $\Delta\theta(0)$ as follows:

$$\frac{b}{W}=\frac{1}{W_0}\left[\frac{\mu}{\gamma U}\right]^{1/2}\alpha I_0(\alpha,U)\frac{1+\alpha^2}{U-1}\ , \quad (3.2')$$

where

$$W_0=\frac{\pi}{\sqrt{48}}\ln\left[\frac{-N(\alpha,U,\epsilon)f(\alpha,U)}{\Delta\theta(0)}\right]\ . \quad (3.2'')$$

Equation (3.2) contains most of the relevant information. Note that the mismatch angle $\Delta\theta(0)$, which is *not* an observable angle,[3] enters the equation via logarithmic function and it weakly depends on external parameters. In what follows we will assume that $W_0\approx$const.[15] For Couder's experiment, W_0 was approximately determined as 2.8.[3]

Motivated by Couder's experiment we now propose the following experiment. For a given two-dimensional Hele-Shaw cell, inject a tiny bubble along the center of the cell and then inject a finite bubble again along the center. Now push the fluid with a rate VW per second. Before the finite bubble touches the tiny one, the relation between V and U will be given by Eqs. (2.21) and (2.24) depending on the size of the bubble. Once it touches the tiny bubble, the velocity U will increase dramatically. We now want to predict the dependence of the enhanced velocity on the wall size W as well as on the area of the bubble J.

Here again we consider three different regimes. In what follows, W_0 is given by (3.2''). The rising velocity will depend on the size of the perturbing bubble but the present model does not take into account this effect because we replace the bubble simply by the cusp. In order for our model to work, the size of the perturbing bubble must be extremely small in comparison to the rising bubble, which is in fact what was observed in the experiment of Maxworthy.[11] In the following discussion the speed U is always assumed to be greater than 2.

A. Saffman-Taylor limit

In this limit $\alpha \to 1$ and $U\lambda = 1$. Substituting these into (2.26) and rearranging the exponential factor, we arrive at the same result for λ and W as was previously obtained in Ref. 3,

$$\frac{b}{W} = \frac{1}{W_0}\left[\frac{\mu U}{\gamma}\right]^{1/2} \frac{\lambda^2}{(1-\lambda)} I_0(1, U=1/\lambda) , \tag{3.3}$$

where $W_0 = W_0(\alpha, U=1/\lambda)$ weakly depends on the external parameters and may be regarded as a constant. In this limit, $W_0 \approx 2.8$.[3]

B. Large but finite bubble limit

In this limit α again approaches 1 but $U\lambda$ is no longer 1 but satisfies (2.10). In this limit the speed of U and W satisfy

$$\frac{b}{W} = \frac{1}{W_0}\left[\frac{\mu U}{\gamma}\right]^{1/2} \frac{1}{U(U-1)} I_0(\alpha=1, U) \times \tanh^{1/2}\left[\frac{J\pi^2 U}{8(U-1)}\right] , \tag{3.4}$$

where $W_0 = W_0(1, 1/U)$. This limit is essentially the same as the Saffman-Taylor limit if one interchanges U and λ by the relation $U = 1/\lambda$.

C. Small bubble limit

This is the most interesting limit. In this case we set $\alpha = 0$ when its contribution is regular. We obtain

$$\frac{b}{W} = \frac{1}{W_0'}\left[\frac{\mu J}{\gamma}\right]^{1/2} \frac{1}{(U-1)^{\frac{3}{2}}} I_0(\alpha=0, U) , \tag{3.5}$$

where

$$\frac{1}{W_0'} = \frac{\pi}{\sqrt{16} W_0(\alpha=0, U)} .$$

Based on (3.5) we find that the speed of the bubble U increases with the wall size W. For a given wall size, the speed U increases as the area of the bubble J increases as $(U-1)^3 \approx J$. We draw a schematic picture in Fig. 3. Once U is selected then the width of the bubble is given by (2.10) which, in the limit $\alpha \to 0$, gives the relation between J, U, and λ as

$$J \approx 4(U-1)U\lambda^2 . \tag{3.5'}$$

A schematic picture of λ as a function of W and J is shown in Fig. 3.

IV. CONCLUSION AND SUMMARY

In this paper we have employed recently developed solvability theory to shed light on the selection mechanism of symmetric finite bubbles in the Hele-Shaw cell. By introducing a cusp at the tip of the bubble we were able to explain the appearance of anomolous bubbles observed in the experiment by perturbing the tip. There are, however, several remaining questions. In a recent report by Zocchi *et al.*,[16] it was discovered that a perturbation caused by wire instead of bubble to the Saffman-Taylor finger produces an asymmetric finger. Recently an attempt[17] was made to understand this new discovery in the light of the solvability theory by assuming that a wire creates a cusp with negative mismatch angle. Here again one can ask the same questions. In the presence of wire along the center, can one observe an asymmetric bubble? Moreover, as was discovered in the experiment of Zocchi *et al.*,[16] if two wires are symmetrically placed along the center of the cell, can one observe a transition from symmetric to asymmetric state? We suspect that the answers to these questions are yes. In Ref. 17 it has been shown that for the Saffman-Taylor finger with a wire at the center, the mismatch angle created by the wire is the same as the one produced by the bubble. We therefore expect that predictions (3.4) and (3.5) will continue to hold for the wire perturbation with a correction of the order of y_0^2, where y_0 is the degree of asymmetry. Recently

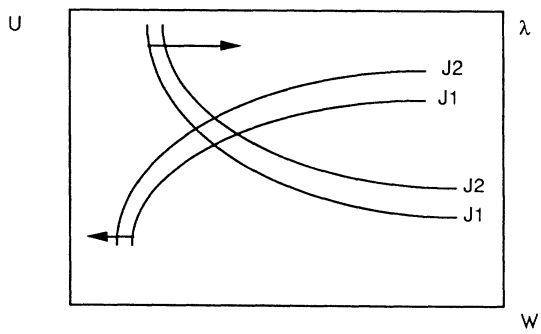

FIG. 3. Dependence of the speed U and the width λ of the bubble in the presence of a cusp at the tip as a function of the wall size and the area of the bubble J in the limit $J \to 0$. The scale is arbitrary and $J_2 > J_1$.

Fearn perturbed the rising bubbles with wire at the center and found that the speed is again dramatically enhanced.[18] His experiment appears to be another convincing proof of solvability mechanism of pattern selection.

ACKNOWLEDGMENTS

This work was supported by the Office of Naval Research and the Petroleum Research Fund administered by the American Chemical Society.

---

*Present address: Department of Physics, Lehigh University, Bethlehem, PA 18015.

[1]D. Bensimon, L. P. Kadanoff, S. Liang, B. I. Shraiman, and C. Tang, Rev. Mod. Phys. **58**, 977 (1986).

[2]B. I. Schraiman, Phys. Rev. Lett. **56**, 2028 (1986); D. C. Hong and J. S. Langer, *ibid.* **56**, 2032 (1986); R. Combescot, T. Dombre, V. Hakim, Y. Pomeau, and A. Pumir, *ibid.* **56**, 2036 (1986).

[3]D. C. Hong and J. S. Langer, Phys. Rev. A **36**, 2325 (1987).

[4]A. Barbieri, D. C. Hong, and J. S. Langer, Phys. Rev. A **35**, 1802 (1987).

[5]M. Ben-Amar and Y. Pomeau, Europhys. Lett. **2**, 307 (1986).

[6]See, for recent developments in this area, J. S. Langer, in *Chance and Matter*, Proceedings of the Les Houches Summer School Session 46, Les Houches, 1986, edited by J. Souletie, J. Vannimenus, and R. Stora (North-Holland, Amsterdam, 1986); D. Kessler, J. Koplik, and H. Levine (unpublished).

[7]G. I. Taylor and P. G. Saffman, Q. J. Appl. Math. **12**, 265 (1959).

[8]P. G. Saffman and G. I. Taylor, Proc. R. Soc. London, Ser. A **245**, 312 (1958).

[9]S. Tanveer, Phys. Fluids **29**, 3537 (1986).

[10]S. Tanveer, Phys. Fluids **30**, 651 (1987).

[11]T. Maxworthy, J. Fluid. Mech. **173**, 95 (1986); see also F. P. Bretherton, *ibid.* **10**, 166 (1961); G. I. Taylor, *ibid.* **10**, 161 (1961).

[12]Y. Couder, N. Gerard, and M. Rabuad, Phys. Rev. A **34**, 5175 (1986).

[13]D. I. Meiron, Phys. Rev. A **33**, 2704 (1986); D. A. Kessler and H. Levine, *ibid.* A **34**, 4980 (1986).

[14]Henry Chou and H. Z. Cummins, Phys. Rev. Lett. **61**, 173 (1988).

[15]The precise value of W_0 can be estimated by including the first-order term in (2.11) and (3.1). In fact it is not difficult to do that and we have carried out the detailed calculation. But we found that the calculation did not produce the same multiplicative factor $N(\alpha, U, \epsilon)$ of Ref. 3 in the Saffman-Taylor limit. This is the reason why we do not try to evaluate $N(\alpha, U, \epsilon)$ precisely in this paper. As was shown in the text, however, the scaling predictions of (2.21) and (2.24) do not depend on $N(\alpha, U, \epsilon)$ but only on the function $Q(\eta)$. Moreover, the predictions of Eqs. (3.3)–(3.5) mainly depend on the factor in the exponential function (3.2) and all the predictions of this paper are correct within the linear approximation.

[16]G. Zocchi, B. Shaw, A. Libchaber, and L. Kadanoff, Phys. Rev. A **35**, 1894 (1987); M. Rabaud, Y. Couder, and N. Gerard, *ibid.* **37**, 5175 (1988).

[17]D. C. Hong, Phys. Rev. A **37**, 2724 (1988); (unpublished).

[18]R. M. Fearn, Phys. Fluids **31**, 238 (1988).